Laminar Boundary-Layer Induced Wave Forces on a Submerged Flat-Plate Hydrofoil

Allen Plotkin*
University of Maryland, College Park, Md.

The two-dimensional, laminar, incompressible high Reynolds number flow of a uniform stream past a submerged flat-plate hydrofoil is analyzed to obtain the wave drag and lift induced on the foil by the effect of viscosity. The viscous effects are modeled by a source distribution on the foil and along the wake centerline whose strength is proportional to the displacement thickness slope. The linearized free-surface boundary condition is satisfied to obtain the wave system. Results are presented for wave drag and lift as a function of Reynolds number, Froude number, and depth to chord ratio.

Introduction

CONSIDER the motion of a body translating at constant speed in an incompressible fluid (water) at or near the free surface. The forces acting on the body may be considered to arise from two physical phenomena. First, the body sets up a system of waves behind it as it moves. The energy necessary to sustain this wave system manifests itself in a drag force on the body called the wave resistance. In general, the analysis uses potential flow theory with the Froude number as the characteristic nondimensional parameter. In addition, a sharp trailing edge can induce a circulatory flow around the body which results in a lift force. Second, the effect of viscosity near the body and in its wake results in a viscous drag force. In general, if flow separation is absent, boundary-layer theory is applicable for large values of the characteristic parameter for viscous flow, the Reynolds number.

The problem of the interaction of the effects of viscosity and free-surface waves is extremely difficult to handle analytically for the three-dimensional flow past a ship. It is well beyond the state-of-the-art to obtain a solution by integration of the Navier-Stokes equations. Even the simplifications involved in using boundary-layer theory for the viscous calculations are not sufficient to render the problem amenable to solution due to the inherent three dimensionality of the flow and the fact that for speeds of interest the flow is mostly turbulent.

Some attempts at studying the interaction problem by an addition of the displacement thickness to the hull were made by Havelock[1] and Wu.[2] Recently, a number of papers have appeared which attempt to model the viscous effects of the wake by distributing vorticity behind the body and working with the inviscid equations. (This idea is somewhat reminiscent of the theory of Prandtl for the flow past a high aspect ratio wing.) Included in this group are the papers of Tatinclaux,[3] Beck,[4] and Kim and Breslin.[5]

Another approach which appears in the literature is to consider the fluid to be completely viscous and study the solution of the Oseen equations which are valid far from the body for any Reynolds number. Dugan[6] considered the two-dimensional flat plate, Lurye[7,8] considered the axisymmetric "singular needle," and Wilson[9] considered singularities accounting for the general force field representative of a ship.

To develop analytical capability for the more accurate predictions of the resistance of bodies moving in or near the free surface, some recent efforts have concentrated on the two-dimensional hydrofoil problem. Gebhardt[10] studied the flow past a submerged hydrofoil and the effect of the wave-modified pressure distribution on the foil boundary layer. Plotkin[11] considered the related modified boundary layer in the wake far behind a symmetric submerged hydrofoil.

Efforts have also been undertaken to obtain higher-order potential flow solutions. Salvesen[12] developed a consistent second-order potential flow theory to calculate the wave resistance on a hydrofoil. Dagan[13] obtained closed-form solutions for the wave drag on a source-generated body but did not consider the induced circulation in his analysis.

The problem considered here is the two-dimensional, laminar, incompressible high Reynolds number flow of a uniform stream past a submerged flat plate hydrofoil at zero angle of attack. The goal is to obtain the wave forces which are induced by the effect of viscosity. The reasons for the consideration of this particular problem are many. First, the complete viscous solution in the absence of the free surface is available. Second, since in the absence of viscosity the plate causes no disturbance, it is possible to calculate separately the wave forces induced by viscosity. Third, it is felt that the viscous effects can be important for thin hydrofoils since the displacement thickness can equal a substantial fraction of the foil thickness.

The model used in this solution can be extended to the turbulent case since essentially the inviscid and viscous solutions are obtained independently.

Viscous Flow Solution

The problem under consideration is the two-dimensional, laminar, incompressible high Reynolds number flow of a uniform stream of speed U past a flat plate of length l aligned parallel to the stream. The plate is located a distance h chord lengths beneath the free surface. All lengths will be normalized by l and all speeds by U. The coordinate system is shown in Fig. 1. x and y are distances along and normal to the plate, respectively, and the origin is located at the leading edge. u and v are the velocity components in the x and y directions.

Consider the complete flowfield in the context of the method of matched asymptotic expansions as expressed,

Received October 15, 1973. This research was supported by the Minta Fund of the University of Maryland. The computer time was donated by the Computer Science Center of the University of Maryland. The author wishes to thank N. Salvesin and M. Wilson of NSRDC, Carderock, Md., for their advice and guidance throughout the course of the research.

Index categories: Boundary Layers and Convective Heat Transfer—Laminar; Hydrodynamics.

*Associate Professor of Aerospace Engineering. Member AIAA.

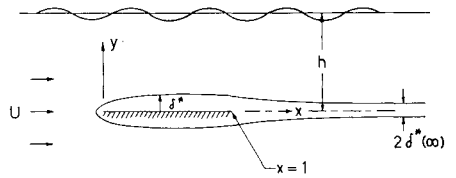

Fig. 1 Coordinate system.

for example, in Chap. 7 of Van Dyke.[14] The first-order inviscid solution is zero since the plate does not disturb the flow. The first-order viscous solution is a boundary-layer solution with zero streamwise pressure gradient (except near the edges) so that the presence of the free surface is not felt. The ordering discussed above is with respect to the small parameter $\epsilon_v = R^{-1/2}$ where the Reynolds number $R = Ul/\nu$ and ν is the kinematic viscosity.

Of interest in this study is the wave system induced by the first-order viscous solution. Conceptually, the stream encounters a semi-infinite body of thickness δ^*, the displacement thickness, which is always small compared to x. A thin-airfoil representation of the body is modeled by a source distribution along the x-axis. The strength per unit length of the distribution, normalized by U, is given by

$$q(x) = 2(d\delta^*/dx) = 2v(x,\infty) \tag{1}$$

$q(x)$ is the only information needed from the viscous solution to be used as input in the consideration of the potential flow.

Plate

The classical Blasius solution is valid on the plate except in the neighborhood of the leading and trailing edges. The treatment of the leading-edge solution is discussed in van de Vooren and Dijkstra.[15] The Blasius solution is invalid in a region of $O(R^{-1})$. Since Ref. 15 treats a semi-infinite flat plate, parabolic coordinates are optimal (see Van Dyke[14]) and the displacement thickness is given by

$$\delta^* = 2\eta R^{-1/2}[x + \eta^2/4R]^{1/2} \tag{2}$$

where $\eta = \eta(x)$ in the leading-edge region and $\eta = 0.8604$, the Blasius value, elsewhere along the plate. Values of η in the leading-edge region are given but their accuracy is questionable and it is consistent for the purposes considered here to use $\eta = 0.8604$ for the leading-edge region as well.

The displacement thickness distribution on the plate, Eq. (2), describes a parabola with vertex at $x = -\eta^2/4R$ and nose radius $a = 2\eta^2 R^{-1}$. Van Dyke[14] shows that the thin-airfoil representation is invalid in the leading-edge region and the extent of this region is $O(a)$ or $O(R^{-1})$. Matched asymptotic expansions are used to improve the solution in this region.

First, the origin is shifted to the leading edge of the parabola by introducing $s = x + \eta^2/4R$. On the surface of the parabola, the exact potential flow solution yields

$$v = \eta R^{-1/2}/(s^{1/2} + \eta^2/Rs^{1/2})$$

For x large compared to R^{-1}, s and x are essentially indistinguishable and therefore on the plate [Eq. (2)]

$$v(x,\infty) = \eta R^{-1/2} x^{-1/2}$$

The rationale for the correction to be introduced is as follows. From the matching principle, $v(x,\infty)$ from the first-order boundary-layer solution is equal to v at $y = 0$ for the second-order potential flow solution (see Van Dyke[14]). From thin-airfoil theory, v at $y = 0$ is equal to v at the parabola surface. In the leading-edge region, trouble exists because of the inadequacy of both boundary-layer and thin-airfoil theory. It is felt to be reasonable therefore to use the correct value of v on the parabola surface in the expression for the source strength in Eq. (1). In the leading-edge region

$$q(s) = 2\eta R^{-1/2}/(s^{1/2} + \eta^2/Rs^{1/2})$$

Since the region of applicability is small, the effect of the leading edge will be modeled by a concentrated singularity placed at the plate's leading edge. The leading-edge region is considered to extend to $s = 5a$ to be consistent with the trailing-edge modeling to be discussed next. At $s = 5a$, the values of v from the corrected and Blasius expressions agree to within 10%.

The strength of the leading-edge singularity, normalized by Ul, is given by

$$Q_{LE} = \int_0^{5a} q(s)ds = 2\eta^2 R^{-1}[2(10)^{1/2} - 2^{1/2}\tan^{-1} 10^{1/2}] \tag{3}$$

On the plate, for $5a \le x \le 1 - 5R^{-3/8}$,

$$q(x) = 2\eta R^{-1/2} x^{-1/2} \tag{4}$$

where the downstream limit of applicability is obtained in the next section.

Trailing-Edge Region

The details of the flow in the neighborhood of the trailing edge are considered by Stewartson[16] and Messiter.[17] The Blasius solution upstream and the Goldstein[18] near-wake solution downstream are invalid in a region of $O(R^{-3/8})$ centered at the trailing edge. The boundary layer is seen to consist of three distinct sublayers (the "triple deck") and the flow in the layer adjacent to the plate is described by the boundary-layer equations with displacement thickness interaction.

Messiter[17] gives the source strength as

$$q(x) = 2\eta R^{-1/2} - 2R^{-1/4} dG_1/dx^* \tag{5}$$

where $x^* = R^{3/8}(x - 1)$. For large negative x^*, $G_1 \to -2.9614x^{*-1}$. For large positive x^*, $G_1 \to 1.2881x^{*1/3} - 2.9614x^{*-1}$. At the trailing edge, G_1 and its first derivative are continuous.

At present, a detailed description of G_1 is not available. Melnik[19] is currently attempting to determine G_1 numerically. Since the details of the solution in the trailing-edge region do not appear to be significant for the computation of the wave forces and since the region under consideration is small for large values of R, the effect of the trailing-edge region will be modeled by a concentrated singularity placed at the trailing edge. The region is considered to extend a distance $5R^{-3/8}$ from the edge—this is chosen to make the correction to the Goldstein[18] solution approximately equal to the Goldstein result itself. This choice should not significantly affect the solution.

The strength of the singularity, normalized by Ul, is

$$Q_{TE} = \int_{1-5R^{-3/8}}^{1+5R^{-3/8}} q(x)dx = 10\eta R^{-7/8} - 1.0181R^{-5/8} \tag{6}$$

It is noted that Messiter[17] points out that his solution is accurate only for $R^{-1/8}$ small. Otherwise neglected terms may become important. In this study, $R \ge 10^6$ will be considered.

The wake solution downstream of the trailing-edge singularity is discussed in Plotkin.[20] In the region $1 + 5R^{-3/8} \le x \le 1.4$, the Goldstein[18] near wake solution is used and it yields

$$q(x) = R^{-1/2}[2\eta - 0.8588(x-1)^{-2/3} - 0.9631(x-1)^{1/3} - 0.8604(x-1) + 0.6865(x-1)^{4/3}] \quad (7)$$

No useful overlap exists between the above solution and the asymptotic far wake solution of Goldstein.[21]

For convenience, a polynomial has been fitted to an "exact" numerical solution of the boundary-layer equations[20] to provide an analytical expression for $q(x)$ in the region $1.4 \leq x \leq 7$. The downstream location of the end of this intermediate wake region is chosen in conjunction with the origin for the far wake solution to provide for a smooth transition from one region to the next. The resulting source strength is

$$q(x) = R^{-1/2}[0.054(x-1)^{-1} - 0.4131(x-1)^{-3/2} + 0.1584(x-1)^{-2} - 0.01879(x-1)^{-5/2}] \quad (8)$$

The far wake solution[21] is

$$q(x) = -0.1759R^{-1/2}x^{-3/2}$$

where the origin of x is undetermined. This origin is chosen at $x = 1.8$ for the reason given above and the source strength for $7 \leq x < \infty$ is

$$q(x) = -0.1759R^{-1/2}(x-1.8)^{-3/2} \quad (9)$$

Potential Flow Solution

To obtain the potential flow solution to second order (in the boundary-layer scheme), the linearized boundary condition at the free surface will be satisfied. The undisturbed free surface is located at $y = h$.

Consider the distributed singularities first-integration from $x = O$ to $x = \infty$ will be understood to exclude the edge regions. The velocity potential ϕ and the stream function ψ are normalized by Ul. In the absence of the free surface, the complex potential is given by

$$f(z) = \phi + i\psi = \int_0^\infty q(\S)\log(z-\S)d\S/2\pi$$

where $z = x + iy$. The complex potential with the gravity images included to satisfy the linearized free surface condition is

$$f(z) = \int_0^\infty q(\S)\log(z-\S)d\S/2\pi + \int_0^\infty q(\S)\log(z-\S-2ih)d\S/2\pi + \int_0^\infty q(\S)I[iF^{-2}(z-\S-2ih)]d\S/\pi$$

where the Froude number $F = U/(gl)^{1/2}$ and

$$I(r) = e^{-r}\int_{-r}^{\infty} e^{-w}dw/w$$

For the calculation of the wave drag, $\psi(x,h)$ as $x \to \infty$ is needed. Far downstream

$$f(z) = \int_0^\infty 2iq(\S)e^{-iF^{-2}(z-\S-2ih)}d\S$$

and

$$\psi(x,h) = 2e^{-h/F^2}[\cos(x/F^2)\int_0^\infty q(\S)\cos(\S/F^2)d\S + \sin(x/F^2)\int_0^\infty q(\S)\sin(\S/F^2)d\S] \quad (10)$$

Similarly, for the concentrated singularities, far downstream we get

$$\psi(x,h) = 2Q_{LE}e^{-h/F^2}\cos x/F^2$$
$$\psi(x,h) = 2Q_{TE}e^{-h/F^2}\cos(x-1)/F^2 \quad (11)$$

(The induced circulation is treated in the next section.)

The problem under consideration possesses two ordering schemes, one for the boundary-layer technique and one for the hydrodynamic technique. Up to this point, reference to first- and second-order results was associated with the boundary-layer ordering scheme with expansion parameter $\epsilon_v = R^{-1/2}$. Use of boundary-layer theory requires ϵ_v to be small.

In this section, the choice to satisfy the linearized free surface boundary condition introduces a new ordering scheme which is discussed in some detail in Salvesen[12] and Dagan.[13] The expansion parameter in this scheme is the ratio of body thickness to submergence depth and is therefore

$$\epsilon_p = R^{-1/2}/h = \epsilon_v/h$$

since $\delta^* = O(R^{-1/2})$. Since first-order theory is used for each ordering scheme, it is consistent to require that ϵ_v and ϵ_p be of the same order. This leads to $h = 0(1)$ or the requirement that the submergence depth be of the order of the chord.

Also, Salvesen[12] states that this ordering implies that

$$ghl/U^2 = 0(1)$$

which leads to $F = 0(1)$. The wave length $\lambda = 2\pi U^2/g$ then is of $0(l)$. Dagan[13] points out that second-order effects dominate for $F \ll 1$.

Induced Circulation

The presence of the free surface introduces asymmetry into the flowfield and the circulation around the plate is nonzero. Strictly speaking, a vorticity distribution exists along the plate whose strength can be obtained by satisfying the plate boundary condition along with the Kutta condition at the trailing edge.

For hydrofoils with angle of attack and camber but no thickness, Strandhagen and Seikel[22] represent the foil circulation by a concentrated vortex placed at the quarter-chord point. Its strength is determined by satisfying the plate condition at the three-quarter chord point. Hough and Moran[23] showed that this approximation is reasonable for a wide range of Froude number. Also, a concentrated vortex model is used in the accurate surface singularity method of Giesing and Smith.[24]

The concentrated vortex representation is used in this analysis. A vortex of strength Γ (measured positive in the clockwise direction and normalized by Ul) is placed at the point (1/4,0). The complex potential for the vortex with the linearized free surface condition satisfied is

$$f(z) = i\Gamma/2\pi[\log(z-1/4) - \log(z-1/4-2ih) - 2I(iF^{-2}(z-1/4-2ih))]$$

To determine Γ, set $v(3/4,0) = 0$. This leads to the equation

$$\Gamma\{2 + 1/(1/2+8h^2) - 2F^{-2}I[iF^{-2}(1/2-2ih)]\} + Q_{LE}\{-2h/(9/16+4h^2) - 2F^{-2}RI[iF^{-2}(3/4-2ih)]\} + Q_{TE}\{-2h/(1/16+4h^2) - 2F^{-2}RI[iF^{-2}(-1/4-2ih)]\} - \int_0^\infty 2hq(\S)d\S/[(3/4-\S)^2+4h^2] - 2F^{-2}R\int_0^\infty q(\S)I[iF^{-2}(3/4-\S-2ih)]d\S = 0 \quad (12)$$

Also, far downstream

$$\psi(x,h) = -2\Gamma\sin F^{-2}(x-1/4)e^{-h/F^2} = 2\Gamma e^{-h/F^2}\sin 1/4F^2\cos x/F^2 - 2\Gamma e^{-h/F^2}\cos 1/4F^2\sin x/F^2 \quad (13)$$

Wave Drag and Lift

The stream function for the singularities evaluated at $y = h$ and for $x \to \infty$ can be written as

$$\psi(x,h) = \sum_1^7 A_i \cos x/F^2 + \sum_1^7 B_i \sin x/F^2 \qquad (14)$$

where, for one segment of the distributed singularities, from Eq. (10)

$$A_i = 2e^{-h/F^2}\int q(\S)\cos\S/F^2 d\S$$
$$B_i = 2e^{-h/F^2}\int q(\S)\sin\S/F^2 d\S \qquad (15)$$

The seven components in Eq. (14) refer to the leading edge, plate, trailing edge, near wake, intermediate wake, far wake, and circulation.

To calculate the wave resistance, Salvesen[12] presents a derivation which requires a streamwise momentum balance in a control volume containing the plate. The control surface consists of the lines $x = -\infty$, $x = x_0 \gg 1$, $y = -\infty$ and the free surface. Care must be taken in adapting the results due to the mass imbalance in the model which represents the presence of the viscous drag.

Conceptually, the displacement surface represents a semi-infinite body whose thickness far downstream is proportional to the viscous drag on the plate. If the body is truly semi-infinite, it would result in the raising of the undisturbed free surface by an amount $2\delta^*(\infty)$ far downstream. In reality, however, it is unlikely that the flow behaves as if a rigid body existed far downstream. The wake is quite diffused and the free surface has modified the streamlines to conform to the wave system. Also, this effect is a manifestation of the viscous drag but it is only the wave drag which is of interest.

In order to use Salvesen's[12] result for the wave drag and to effectively eliminate the viscous drag from consideration, a fictitious mass influx is distributed along $y = -\infty$ to balance the mass outflow $2U\delta^*$ through the downstream boundary of the control surface. This allows the undisturbed free surface to remain at $y = h$ and cancels the streamwise momentum flux due to the mass imbalance.

Salvesen[12] has shown that the wave resistance is given by

$$R_w = \rho g l^2\left[\left(\sum_1^7 A_i\right)^2 + \left(\sum_1^7 B_i\right)^2\right]/4 \qquad (16)$$

where ρ is the fluid density. A wave drag coefficient is defined as

$$C_w = \frac{R_w}{\rho g l^2} = \left[\left(\sum_1^7 A_i\right)^2 + \left(\sum_1^7 B_i\right)^2\right]/4 \qquad (17)$$

The lift force on the plate is given by

$$L = \rho U^2 l\Gamma - \rho U^2 l\Gamma^2/4\pi h + \rho F^{-2}\Gamma^2 U^2 l e^{-2hF^{-2}} Ei(2hF^{-2})/\pi$$

and a lift coefficient is defined as

$$C_L = 2\Gamma - \Gamma^2/2\pi h + 2F^{-2}\Gamma^2 e^{-2hF^{-2}} Ei(2hF^{-2})/\pi = \frac{L}{\rho U^2 l/2} \qquad (18)$$

where Ei is defined in Ref. 25.

The A_i's and B_i's will now be obtained for the various flow components.

Leading Edge

From Eqs. (3, 11 and 14),

$$A_1 = 4\eta^2 R^{-1} e^{-h/F^2}(2(10)^{1/2} - \tan^{-1} 10^{1/2})$$
$$B_1 = 0$$

Plate

Equations (4) and (15) are used. The integral in Eq. (15) is split into two parts

$$\int_{5a}^{1-5R^{-3/8}} = \int_{5a}^{1} - \int_{1-5R^{-3/8}}^{1}$$

After some manipulation and keeping terms of order equal to or lower than $0(R^{-1})$, the following is obtained

$$A_2 = -4\eta^2 R^{-1}(2(10)^{1/2})e^{-h/F^2} + 4\eta R^{-1/2}(2\pi)^{1/2} F e^{-h/F^2} C[(2/\pi)^{1/2}F^{-1}] - 20\eta R^{-7/8} e^{-h/F^2}\cos F^{-2}$$

$$B_2 = 4\eta R^{-1/2}(2\pi)^{1/2} F e^{-h/F^2} S[(2/\pi)^{1/2}F^{-1}] - 20\eta R^{-7/8} e^{-h/F^2}\sin F^{-2}$$

where C and S are Fresnel integrals and are defined and tabulated in Chap. 7 of Abramowitz and Stegun.[25]

It is noted that in adding $A_1 + A_2$ the first term in A_1 is cancelled and the leading-edge singularity acts as a sink. This is consistent with the leading-edge correction discussed in Van Dyke[14] in which the flow speed is effectively increased in the leading-edge region.

Trailing Edge

From Eqs. (6, 11, and 14),

$$A_3 = 40\eta R^{-7/8} e^{-h/F^2}\cos F^{-2} - 4(1.0181)R^{-5/8} e^{-h/F^2}\cos F^{-2}$$

$$B_3 = 40\eta R^{-7/8} e^{-h/F^2}\sin F^{-2} - 4(1.0181)R^{-5/8} e^{-h/F^2}\sin F^{-2}$$

Note that the third terms in the plate expression cancel half of the first terms in the trailing edge expressions. Also note that the highest order contribution is $0(R^{-5/8})$ and that this is important compared to $0(R^{-1/2})$.

Near Wake

Equations (7) and (15) are used. Take

$$q(\S) = 2\eta - g(\S)$$

Then

$$A_4 = -20\eta R^{-7/8} e^{-h/F^2}\cos F^{-2} + 4\eta R^{-1/2} F^2 e^{-h/F^2}(\sin 1.4F^{-2} - \sin F^{-2}) - 2R^{-1/2} e^{-h/F^2}\int_{1+5R^{-3/8}}^{1.4} g(\S)\cos\S/F^2 d\S$$

$$B_4 = -20\eta R^{-7/8} e^{-h/F^2}\sin F^{-2} - 4\eta R^{-1/2} F^2 e^{-h/F^2}(\cos 1.4F^{-2} - \cos F^{-2}) - 2R^{-1/2} e^{-h/F^2}\int_{1+5R^{-3/8}}^{1.4} g(\S)\sin\S/F^2 d\S$$

Note that the first terms cancel the remaining half of the first terms in the trailing edge expressions. Only the terms of $0(R^{-5/8})$ are left.

Intermediate and Far Wake

These results are obtained by using Eqs. (9) and (15), respectively.

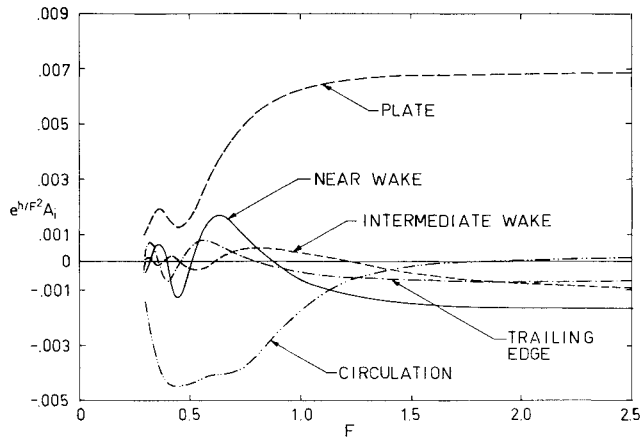

Fig. 2 Contribution to A_i from individual flow components.

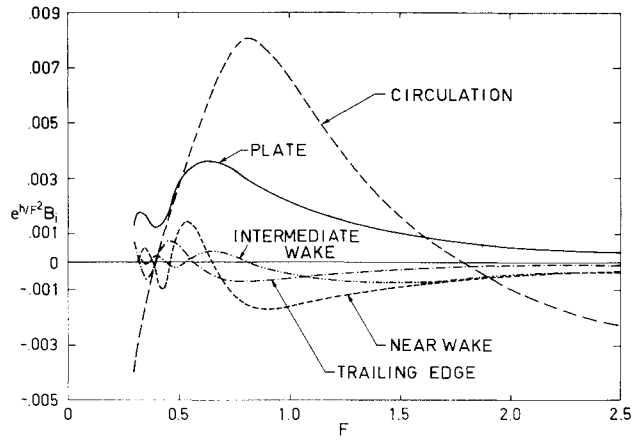

Fig. 3 Contribution to B_i from individual flow components.

Circulation

From Eqs. (13) and (14),

$$A_7 = 2\Gamma e^{-h/F^2} \sin 1/4F^2$$

$$B_7 = -2\Gamma e^{-h/F^2} \cos 1/4F^2$$

Results and Discussion

In order to calculate the force coefficients, it is necessary to evaluate the Fresnel integrals $C(r)$ and $S(r)$ and the real and imaginary parts of the function $I(r)$. These quantities are tabulated in Ref. 25 but it is more convenient, especially since $I(r)$ appears in a numerical integration, to have series representations available. These are also given in Ref. 25 as follows:

$$C(r) = \sum_{n=0}^{\infty} (-1)^n (\pi/2)^{2n} r^{4n+1}/(2n)!(4n+1)$$

$$S(r) = \sum_{n=0}^{\infty} (-1)^n (\pi/2)^{2n+1} r^{4n+3}/(2n+1)!(4n+3)$$

$$I(r) = -e^{-r}\left(\gamma + \log r + i\pi + \sum_{1}^{\infty} r^n/nn!\right)$$

where γ, Euler's constant is 0.57721566. Also, if $|Rr| > 10$ or $|Ir| > 10$, then $I(r) \pm 0.711093/(-r + 0.415775) + 0.2781518/(-r + 2.29428) + 0.010789/(-r + 6.29)$. All of the integration is performed numerically using Simpson's 1/3 rule.

To calculate the wave drag coefficient, C_w, from Eq. (17), the coefficients A_i and B_i must be determined. To evaluate the contributions of the various flow components, recognition will be taken of the fact that certain terms cancel in the summations of the A_i and B_i and the effect of the flow components is then given without the cancelled terms.

The contributions to A_i are shown in Fig. 2 and to B_i in Fig. 3. Some explanation must be given to the manner in which these results are displayed. The Reynolds number dependence is both explicit and implicit. The lowest order Reynolds number contribution to the coefficients is $0(R^{-1/2})$ with the trailing-edge region contributing a term of $0(R^{-5/8})$. Terms of both these orders appear in the circulation. It is felt that the nature of the Reynolds number dependence can be seen by an inspection of the equations for the coefficients and therefore all the plotted results are given for a representative value of $R = 10^6$.

Results are given for a Froude number range $0.3 \leq F \leq 3$. It is noted that all terms are proportional to e^{-h}/F^2 and that the only other depth dependence appears in the circulation term. To keep the results general, e^{-h}/F^2 is factored out even though it is F dependent and $h = 1$ is selected for the circulation term. For $h > 1$, the circulation term has a smaller contribution. The leading-edge contribution, which is $0(R^{-1})$, is clearly too small to appear in the figures. Also, the contribution from the far wake is too small to be shown in the figures. The maximum magnitude of either A_6 or B_6 is approximately $0.1e^{-h}/F^2 R^{-1/2}$.

From the figures, it is seen that the flow consists of three main components, the plate, the wake, and the circulation. In general, the wake tends to reduce the effect of the plate and except in the low F range, the circulation tends to complement the effect of the plate. It is noted that except for the oscillations at low F, the contributions of most of the flow components tend to become independent of Froude number as the Froude number increases.

To assess more carefully the contributions of the various flow components to the overall wave drag, Figs. 4–6 must be studied. In Fig. 4, the wave drag coefficient due solely to the plate contribution is given. This term is $0(R^{-1})$. Curves are presented for $h = 1$, 2, and 3 and $R = 10^6$. It can be seen that the factor e^{-h}/F^2 provides maximum damping for small values of F and that C_w is monotonically increasing with F.

Figure 5 presents the wave drag contribution from all flow components except the circulation. Curves are again presented for $h = 1$, 2, and 3 and $R = 10^6$. This figure, when studied in conjunction with Fig. 4, gives the effect of the inclusion of the viscous wake in the analysis. It is seen that the general shape of the curves is unchanged but that the magnitude of the resistance has been reduced by approximately a factor of four.

Figure 6 shows the wave drag coefficient for the complete flowfield for $h = 1$, 2, and 3 and $R = 10^6$. This figure demonstrates the contribution of the induced circulation to the wave drag. It is noted that this contribution depends more strongly on depth than the others since Γ de-

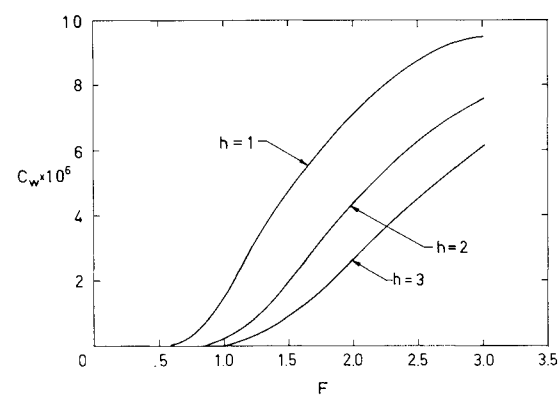

Fig. 4 Plate contribution to wave drag coefficient.

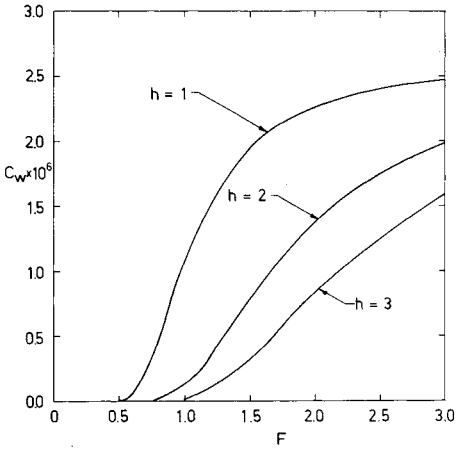

Fig. 5 Wave drag coefficient minus contribution from circulation.

creases with h. This can be clearly seen in the results for $h = 2$ and $h = 3$ since C_w changes only slightly from Fig. 5 to Fig. 6. For $h = 1$, the circulation clearly complements the plate results and returns the wave drag to 50% of its value for the plate alone. Also, for $h = 1$, the addition of the circulation term gives the wave drag curve the familiar non-monotonic increase with F.

The lift coefficient, C_L, from Eq. (18), is shown in Fig. 7 for $h = 1$, 2, and 3 and $R = 10^6$. It is seen that C_L is strongly depth dependent. The lowest order term in C_L is $0(R^{-1/2})$ so that $C_L/C_w = 0(R^{1/2})$ for $R \to \infty$ for the flat plate hydrofoil. It is noted that the curves of C_L vs F for different values of h have the same general shape as the curves presented in Ref. 24 for the depth effect on C_L for flat-plate hydrofoils at angle of attack. The curves possess minimums which occur at larger values of F for larger values of h. Viscosity can be thought of as inducing an angle of attack on the hydrofoil, one which is negative for low values of F and becomes positive for larger values of F.

A comment is in order here about the model used for the wake. Wu[2] felt that the determination of a "proper" wake modeling was one of the more difficult aspects of this interaction problem. He raised the question of the appropriateness of considering a semi-infinite body to represent the wake and mentioned the alternative of some type of mathematical modeling which reduces the thickness to zero at some finite distance downstream of the trailing edge. This question has not been answered here but some pertinent observations can be made.

From a mathematical point of view, Van Dyke[14] demonstrates that in the limit as $R \to \infty$, the second-order potential flow represents the flow past a semi-infinite body formed by adding the displacement thickness to the body surface. The model used in this analysis is a traditional

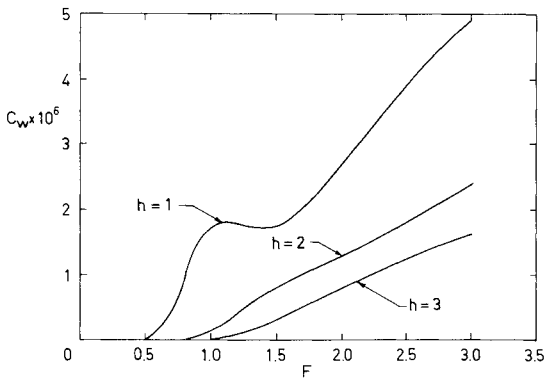

Fig. 6 Wave drag coefficient.

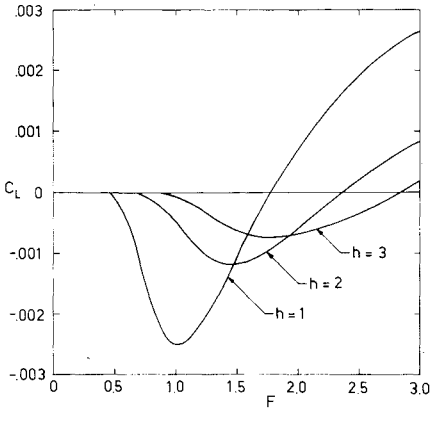

Fig. 7 Lift coefficient.

one for the aerodynamicist and appears many times in the literature (see Spence[26]). The value of δ^* as predicted from the viscous analysis is used to model the wake. It should also be noted, however, that many current analyses which consider the inclusion of the displacement effect in airfoil calculations resort, perhaps out of necessity, to a termination of the wake shortly behind the trailing edge.

It is seen from this analysis that the contribution to the wave drag from the far wake ($x > 7$) is essentially negligible compared to that from the rest of the wake. This indicates that the present results could be duplicated with a different wake model, notably one of finite extent. This type of modeling would eliminate the wake mass imbalance and related problems discussed earlier. It is felt that experimental results should be used to guide the analyst in the task of modeling the wake so as to best reproduce the generated wave system.

A comment is also in order about the order of magnitude of the effects determined in this analysis. The lowest order term in C_w is $0(R^{-1})$ and in C_L is $0(R^{-1/2})$. Wu[2] points out that for a body of finite thickness (or similarly for a foil with angle of attack), the terms above which are due to the effect of viscosity alone would not be the most important but would be negligible compared to the terms due to the interaction of the viscosity-induced wave system with the body-induced wave system. For example, if the first-order body-induced terms in C_w are 0(1), then the interaction term would be $0(R^{-1/2})$. Also, in Refs. 12 and 13 it is assumed that viscous terms are less important than potential flow terms that are of higher order in the thickness to depth ratio. For a particular body, especially a thin one, this analysis is a step along the way to putting one in a position to verify or disprove this assumption.

Finally, a word of caution is given with respect to extending the results of this analysis to higher order. It is recalled that this problem possesses two ordering schemes and the possibility exists that the analyst may not be able to alternate back and forth between the viscous and potential flow solutions, one order at a time. Also, the asymmetry in the first-order solution leads to the necessity of locating the wake centerline for any extensions of the theory. In the absence of the free surface, the unknown-in-advance wake curvature and location are important in the solution as demonstrated by Spence.[27] The presence of the free surface will no doubt add a wavy character to the wake location which can only further complicate the analysis.

References

[1]Havelock, T. H., "Calculations Illustrating the Effect of Boundary Layer on Wave Resistance," *The Collected Papers of Sir Thomas Havelock on Hydrodynamics*, edited by C. Wigley, ONR/ACR-103, U.S. Government Printing Office, Washington, D.C., 1963, pp. 528–535.

[2]Wu, T. Y., "Interaction Between Ship Waves and Boundary Layer," *Proceedings of the International Seminar on Theoretical Wave Making Resistance,* Vol. III, University of Michigan, Ann Arbor, Mich., 1963, pp. 1263–1287.

[3]Tatinclaux, J. C., "Effect of a Rotational Wake on the Wave-making Resistance of an Ogive," *Journal of Ship Research,* Vol. 14, No. 2, 1970, pp. 84–99.

[4]Beck, R. F., "The Wave Resistance of a Thin Ship with a Rotational Wake," *Journal of Ship Research,* Vol. 15, No. 3, 1971, pp. 196–216.

[5]Kim, C. H. and Breslin, J. P., "A Theoretical Study of the Effect of Viscosity on Wave Resistance," Report SIT-DL-72-1596, 1972, Davidson Lab., Stevens Inst. of Technology, Hoboken, N.J.

[6]Dugan, J. P., "Viscous Drag of Bodies Moving near a Free Surface," *Physics of Fluids,* Vol. 12, No. 1, 1969, pp. 1–10.

[7]Lurye, J. R., "Interaction of Free-Surface Waves with Viscous Waves," *Physics of Fluids,* Vol. 10, No. 2, 1968, pp. 261–265.

[8]Lurye, J. R., "Wave Height and Wave Resistance in the Presence of a Viscous Wake," *Physics of Fluids,* Vol. 16, No. 6, 1973, pp. 750–760.

[9]Wilson, M. B., "A Havelock-Oseen Theory for Ship Resistance," presented at the Thirteenth International Congress of Theoretical and Applied Mechanics, Moscow, USSR, 1972.

[10]Gebhardt, J. C., "The Skin Friction of a Hydrofoil Near a Free Surface," Report 08368-1-F, 1968, Dept. of Naval Architecture and Marine Engineering, University of Michigan, Ann Arbor, Mich.

[11]Plotkin, A., "The Symmetric Far Wake Behind a Cylinder Beneath the Free Surface, *Journal of Hydronautics,* Vol. 8, No. 1, Jan. 1974, pp. 41–43.

[12] Salvesen, N., "On Second-Order Wave Theory for Submerged Two-Dimensional Bodies," ONR Sixth Naval Hydrodynamics Symposium, ONR/ACR-136, Washington, D.C., 1966, pp. 595–636.

[13]Dagan, G., "A Study of the Nonlinear Wave Resistance of a Two-Dimensional Source Generated Body," TR 7103-2, 1972, Hydronautics, Inc., Laurel, Md.

[14]Van Dyke, M., *Perturbation Methods in Fluid Mechanics,* Academic Press, New York, 1964.

[15]van de Vooren, A. I. and Dijkstra, D., "The Navier-Stokes Solution for Laminar Flow Past a Semi-Infinite Flat Plate," *Journal of Engineering Mathematics,* Vol. 4, No. 1, 1970, pp. 9–27.

[16]Stewartson, K., "On the Flow Near the Trailing Edge of a Flat Plate II," *Mathematika,* Vol. 16, 1969, pp. 106–121.

[17]Messiter, A. F., "Boundary-Layer Flow Near the Trailing Edge of a Flat Plate," *SIAM Journal on Applied Mathematics,* Vol. 18, No. 1, 1970, pp. 241–257.

[18]Goldstein, S., "Concerning Some Solutions of the Boundary Layer Equations in Hydrodynamics," Proceedings of the Cambridge Philosophical Society, Vol. 26, 1970, pp. 1–30.

[19]Melnik, R. E., private communication, July 1973, Palm Springs, Calif.

[20]Plotkin, A., "Calculation of Displacement Thickness Slope Downstream of the Flat Plate Trailing-Edge Singularity Using Goldstein's Solutions," unpublished note.

[21]Goldstein, S., "On the Two-Dimensional Steady Flow of a Viscous Fluid Behind a Solid Body," *Proceedings of the Royal Society (London),* Vol. A142, 1933, pp. 545–562.

[22]Strandhagen, A. G. and Seikel, G. R., "Lift and Wave Drag of Hydrofoils," *Proceedings of the Fifth Midwestern Conference on Fluid Mechanics,* University of Michigan Press, Ann Arbor, Mich., 1957, pp. 351–364.

[23]Hough, G. R. and Moran, J. P. "Froude Number Effects on Two-Dimensional Hydrofoils," *Journal of Ship Research,* Vol. 13, No. 1, 1969, pp. 53–60.

[24]Giesing, J. P. and Smith, A. M. O., "Potential Flow about Two-Dimensional Hydrofoils," *Journal of Fluid Mechanics,* Vol. 28, No. 1, 1967, pp. 113–129.

[25]Abramowitz, M. and Stegun, I. A., *Handbook of Mathematical Functions,* National Bureau of Standards Applied Mathematics Series 55, 1964.

[26]Spence, D. A., "Prediction of the Characteristics of Two-Dimensional Airfoils," *Journal of the Aeronautical Sciences,* Vol. 21, No. 9, 1954, pp. 577–587, 620.

[27]Spence, D. A., "Wake Curvature and the Kutta Condition," *Journal of Fluid Mechanics,* Vol. 44, 1970, pp. 625–636.

APRIL 1974 J. HYDRONAUTICS VOL. 8, NO. 2

Effect of a Wavy Bottom on Kelvin-Helmholtz Instability

A. Mitra* and M. D. Greenberg†
University of Delaware, Newark, Del.

The linearized Kelvin-Helmholtz free surface instability is investigated for the case where the upper fluid is bounded and streaming with a velocity U, and the lower fluid is at rest and bounded by a sinusoidal bottom. A vortex sheet model is formulated, and a perturbation solution in the bottom amplitude is developed in which the time variable is strained. For any given set of physical parameters, it is found that flat-bottom stability implies wavy-bottom stability, except for a discrete set of exceptional wave numbers, for which no conclusion regarding stability can be drawn from the present analysis.

Nomenclature

A = the difference ξ-x
$\mathbf{A}_r$ = coefficient matrix, see Eq. (26)
B = $\eta(x, t) - \eta(\xi, t)$
$\mathbf{C}_n{}^r$ = column vector, see Eq. (26)
d = mean undisturbed depth
g = vorticity perturbation, see Eq. (8)
g = acceleration of gravity
$\mathbf{g}$ = column vector $(g, h, \bar{g})$ transpose
$\mathbf{g}_j$ = jth coefficient in λ-expansion of $\mathbf{g}$, see Eq. (16)
$\mathbf{G}_n{}^r$ = column vector of g, h, $\bar{g}$ amplitudes, see Eq. (21)
h = free surface perturbation, see Eq. (8)
i = $(-1)^{1/2}$ and dummy index
I_j = velocity perturbations (j = 1, 2, 3), see Eqs. (9–12)
$I_i{}^j$ = jth coefficient in λ-expansion of I_i, see Eq. (18)
${}^rI_i{}^n$ = the part of $I_i{}^n$ involving $\mathbf{g}_r$
k = wave number
p = pressure

Received July 9, 1973; revision received November 6, 1973. The authors are grateful to the University of Delaware Research Foundation and the Geography Branch of the Office of Naval Research for their support.

Index categories: Oceanography, Physical and Biological; Propulsion System Hydrodynamics.

*Graduate Student, Department of Mechanical and Aerospace Engineering.

†Associate Professor, Department of Mechanical and Aerospace Engineering.